

Adaptive spraying decision system for plant protection unmanned aerial vehicle based on reinforcement learning

Ziyuan Hao¹, Xinze Li¹, Chao Meng¹, Wei Yang^{1,2*}, Minzan Li^{1,2}

(1. Key Laboratory of Smart Agriculture System Integration, Ministry of Education, China Agricultural University, Beijing 100083, China;

2. Key Laboratory of Agricultural Information Acquisition Technology, Ministry of Agriculture and Rural Affairs, China Agricultural University, Beijing 100083, China)

Abstract: To solve the problem of lacking scientific guidance in aerial pesticide application, this study introduced an adaptive spraying decision system (ASDS) for Unmanned Aerial Vehicle (UAV) spraying to guide the operators of plant protection UAVs to set reasonable spraying parameters under complicated environment. The minimum applied volume rate, proper spraying velocity, spraying height, and initial droplet size were recommended by the ASDS. The key factor of the decision system is the decision model of reinforcement learning based on the actor-critic neural network. In specific, the field experimental data were used to train the critic and actor networks, which made the model adaptive to optimize the output of spraying parameters. Compared with the conventional spraying parameters, the spraying parameters recommended by the ASDS had a positive impact on wheat parcels. The decision results of the ASDS showed that the spraying volume rate was lower in the blocks with a small leaf area index. In addition, the spraying volume rate for the whole parcel was reduced by 14%. After UAV spraying, the uniformity of the droplet deposition in the ASDS parcel was better than that in the conventional parcel. Moreover, the penetrability of the droplets and the control efficacy for the brown wheat mite *Petrobia latens* (Muller) were similar in the two parcels. The ASDS can recommend the optimal spraying parameters to minimize pesticide application.

Keywords: unmanned aerial vehicle, spraying parameters, decision, reinforcement learning, droplet deposition

DOI: 10.25165/j.ijabe.20221504.6929

Citation: Hao Z Y, Li X Z, Meng C, Yang W, Li M Z. Adaptive spraying decision system for plant protection unmanned aerial vehicle based on reinforcement learning. Int J Agric & Biol Eng, 2022; 15(4): 16–26.

1 Introduction

Pesticide application is an essential part of crop production in the field, and the biological effects of pesticides are affected by the droplet deposition (the volume of droplets deposited per unit area, $\mu\text{L}/\text{cm}^2$) after spraying on the canopy. Spraying pesticides to control diseases and insect pests is a complex process, and the effect of spraying pesticides is closely related to the spraying technology used^[1]. Currently, the plant protection machines used to prevent and control crop pests and diseases include plant protection unmanned aerial vehicles (UAVs), ground mechanical sprayers, and manual knapsack sprayers^[2]. In recent years, small- and medium-sized farms are the main body of field crop production in China; meanwhile, the labor shortage has intensified^[3]. The use of manual knapsack sprayers is labor-intensive and time-consuming, and the ground mechanical sprayers inevitably damage ground plants. The high spraying efficiency and good mobility of UAVs make them suitable for the current agricultural production in China and have become the main means

of plant protection^[4].

While UAVs are widely used, a series of related problems have also emerged. Currently, scientific guidance for the settings of UAV spraying parameters is lacking, and most UAV operators have strong subjectivity in setting parameters. Therefore, the droplets of pesticides may not be accurately deposited on the crop canopy, which could affect the control efficacy of pesticides and cause pesticide waste^[5]. In view of this situation, relevant studies have been carried out. Qin et al.^[6] studied the effects of UAV spraying height and spraying velocity on the droplet deposited in rice canopy and found that the best droplet deposition effect was achieved when the height was 1.5 m and the velocity was 5 m/s. Meanwhile, the control efficacy of UAVs against paddy rice plant hopper has significant advantages. Chen et al.^[7] studied the effects of different droplet sizes of UAV nozzle (i.e., 95.21 μm , 121.43 μm , 147.28 μm , and 185.09 μm , respectively) on droplet distribution and found that large droplets have good penetration effects^[7]. After spraying wheat with different volumes (i.e., 9.0 L/hm², 16.8 L/hm², and 28.1 L/hm²), Wang et al.^[8] found that UAV spraying at a high volume with coarse nozzles has the same control efficacy against wheat aphid and powdery mildew as the electric air-pressure knapsack sprayer. At present, the studies give suitable UAV spraying parameters in specific scenarios that are mature. However, the droplet deposition effect and the control efficacy of pesticides are affected not only by UAV parameters but also by environmental factors. The deposition position of droplets, the retention of droplets on the leaves, and the evaporation speed of droplets are affected by the wind speed, humidity, and temperature in the environment^[9,10]. In view of the changing field environment, dynamic parameter setting suggestions must be

Received date: 2021-07-26 **Accepted date:** 2022-01-10

Biographies: Ziyuan Hao, PhD candidate, research interests: precision agriculture, Email: haoziyuan@cau.edu.cn; Xinze Li, MS, research interests: agricultural informatization, Email: 744433332@qq.com; Chao Meng, PhD candidate, research interests: agricultural engineering, Email: mc6663@cau.edu.cn; Wei Yang, PhD, Associate Professor, research interests: agricultural informatization, Email: cauyw@cau.edu.cn; Minzan Li, PhD, Professor, research interests: precision agriculture, Email: limz@cau.edu.cn.

*Corresponding author: Wei Yang, PhD, Associate Professor, research interests: agricultural informatization. China Agricultural University, Beijing 100083, China. Tel: +86-13810270311, Email: cauyw@cau.edu.cn.

provided to guide UAV operators in spraying pesticides. Therefore, a UAV decision-making system is necessary to realize the adaptive adjustment of spraying parameters.

At present, the decision system for the ground mechanical sprayers is mature. A decision support system for the ground mechanical sprayers was developed by Gil et al.^[11] to determine the optimal volume rates based on the leaf wall area of vineyards. Meanwhile, other working parameters were recommended. Tackenberg et al.^[12] studied a variable-rate fungicide application technology based on a camera sensor and found that it can provide a reasonable spraying volume of the field boom sprayer according to the leaf area index (LAI) and biomass of wheat to minimize pesticide application. Pesticide reduction is a worldwide concern^[13]. Most existing decision-making systems try to reduce the use of pesticides according to the growth of crops while ensuring the control effect. In addition, some diseases will be prevented in advance^[14] when the diseases have not occurred, and it is difficult for UAVs to spray pesticides according to the degree of the diseases. In this case, the growth of crops needs to be mainly considered in the decision-making process, and the LAI is an important index^[15]. To reduce pesticide use and guide UAV spraying scientifically, the decision system in this study will recommend the minimum applied volume rate and reasonable other spraying parameters (i.e., initial droplet size, UAV spraying speed, and UAV spraying height) according to the LAI of the crop and the environmental impact creatively. The decision-making process can be simplified as a dynamic programming model. The optimal decision results in this study need to change with the complex and changeable environment, and the traditional dynamic programming model cannot flexibly adjust the decision results. In recent years, reinforcement learning (RL), as a new artificial intelligence algorithm, has been widely used in decision-making and attracted attention in the field of agriculture^[16]. The RL algorithm is a learning algorithm that uses agents to map from the input to the output of the model. The RL algorithm can learn continuously during interaction with the environment to optimize the performance index function and the decision strategy. The RL algorithm based on the actor-critic network structure is commonly used and has great advantages in approaching the optimal strategy; therefore, it is recognized and applied widely^[17].

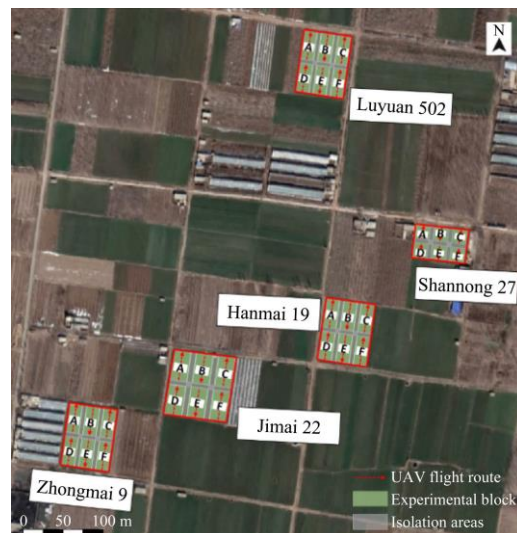
In this study, wheat was applied as the research subject. A spraying decision model was designed based on field data and the decision model of RL based on the actor-critic neural network, and then an adaptive spraying decision system (ASDS) was developed by applying an Android smart device and a micro-computer Raspberry Pi. Finally, the ASDS was evaluated from the perspectives of the deposited droplets effect and the control efficacy of *Petrobria latens* in wheat field.

2 Materials and methods

2.1 Experimental plots

Experiments were carried out in a commercial wheat plantation zone in Tai'an City, Shandong Province, China (36°15'38.70324"N and 116°36'35.8884"E), which was located in North China. Two experimental tasks were performed on the same farm that had the same cropping pattern for wheat in different years. A database for the decision model was established in experimental task 1. Five parcels (Figure 1) containing five wheat varieties were selected: Zhongmai 9 (field size was 70×88 m²), Luyuan 502 (field size was 64×86 m²), Hanmai 19 (field size was 76×85 m²), Shannong 27 (field size was 70×47 m²), and Jimai 22 (field size was 88×93 m²).

The agronomic traits of different wheat varieties were different, and the LAI values of the same growth stage had differences. In experimental task 2, the pesticide was sprayed according to the application recommendations of the ASDS, and the effect of spraying was evaluated. The experiment was carried out in three parcels, namely, the ASDS parcel (field size was 188×100 m²), the conventional parcel (field size was 160×96 m²), and the blank parcel (field size was 32×55 m²) (Figure 2), in which the wheat varieties were all Luyuan 502.



Note: A, B, C, D, E, and F in the figure represent the experimental blocks in each experimental parcel.

Figure 1 Sketch map of the parcels in experimental task 1

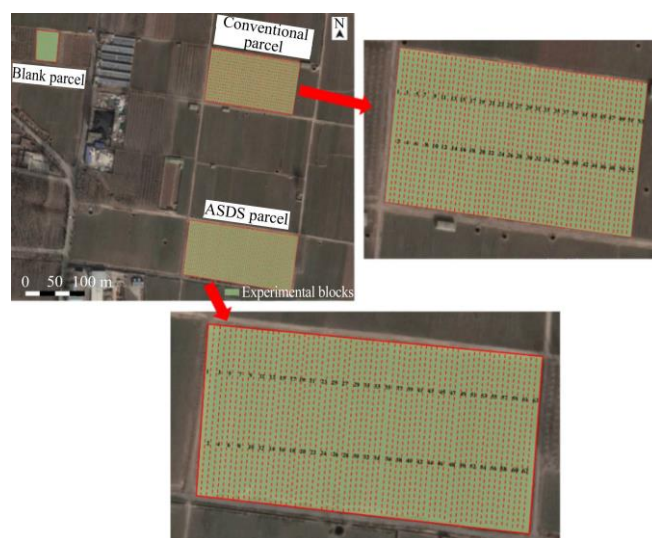


Figure 2 Sketch map of the parcels in experimental task 2

2.2 Experimental treatments

The wheat growth characteristics of different wheat ridges in the experimental parcels were different, and the growth of the same ridge was similar. In experimental task 1, each of the five experimental parcels was divided into six equal-area blocks (Figure 1). Therefore, the UAVs sprayed a row of wheat in each block according to the direction of the ridge. The isolation areas 10 m wide were set up between different blocks to prevent the UAV spray experiments in different blocks from interfering with each other. The experimental period was from March 2020 to June 2020. Experiments were conducted in four growth stages of wheat that were 32, 39, 45, and 59 according to the Biologische Bundesanstalt, Bundessortenamt, and Chemical industry (BBCH)-scale^[18]. Six different applied volume rates were applied

to six different blocks in each parcel (Table 1). In addition, the initial droplet size, UAV spraying velocity, and UAV spraying height must be considered because the different combinations of these operating parameters affect the droplet deposition effect^[10,19,20]. The XAG P20 plant protection UAVs with high-speed atomizing nozzles (XAIRCRAFT, China) were used for spraying, and the value levels of some spraying parameters are listed in Table 2. The number of tests needed for a comprehensive experiment was too many. Therefore, an L32(6³5⁴) orthogonal table was designed based on the Pairwise Independent Combinatorial Testing (PICT) tool (Microsoft, USA) and parameters in Table 2 to obtain 32 experimental combinations and was applied in experimental task 1. Finally, 32 spraying tests were carried out in each block of each parcel.

Table 1 Treatments of applied volume rates in different blocks

Experimental blocks	Applied volume rate/L·hm ⁻²
A	6.0
B	9.0
C	12.0
D	15.0
E	18.0
F	21.0

Table 2 Value levels of UAV spraying parameters

Parameters	Levels					
	1	2	3	4	5	6
Initial droplet size $d/\mu\text{m}$	105	120	135	150	165	--
UAV spraying velocity $v/\text{m}\cdot\text{s}^{-1}$	2	3	4	5	6	7
UAV spraying height h/m	1	2	3	4	5	--

The winter wheat region of North China where the experiment was located was an endemic area of the brown wheat mite *P. latens* (Muller)^[21]. Experimental task 2 was carried out on April 2, 2021. In this year, the diseases of wheat were not serious, and only Luyuan 502 was found infected with *P. latens*. The average number of *P. latens* per wheat plant in the three parcels was more than 6, and 5% avermectin was sprayed to control *P. latens*. The ASDS parcel was divided into 63 blocks according to the direction of the ridge to achieve variable spraying on the basis of the LAI; in addition, the width of each block was 3 m because the UAV spraying width was set at 3 m in the experiments (Figure 2). This block was also convenient to operate the UAVs to spray according to the parameters guidance of the ASDS. Meanwhile, the conventional parcel was divided into 53 equal 3-meter-wide blocks according to the direction of the ridge, and a single parameter combination (UAV spraying height was 2 m, UAV spraying velocity was 7 m/s, initial droplet size was 110 μm , and applied volume rate was 15.0 L/hm²) was used to spray pesticide in the conventional parcel according to the habits of UAV operation professionals^[22]. In addition, the blank parcel did not have any treatment and played a contrasting role. Before spraying and on the 1st, 3rd, and 7th days after control, the pest situation of the three parcels was investigated. The diagonal 5-point sampling method was used, and 20 wheat plants were selected at each point to investigate the number of *P. latens* that was used to calculate the reduced rate of *P. latens* population (Equation (1)) and control efficacy (Equation (2))^[23].

$$R = \frac{P_0 - P_1}{P_0} \times 100\% \quad (1)$$

where, R is the reduced rate of *P. latens* population, %; P_0 is the

number of *P. latens* before spraying and P_1 is the number of *P. latens* after spraying.

$$C = \frac{PT - CK}{100 - CK} \times 100\% \quad (2)$$

where, C is the control efficacy, %; PT is the reduced rate of *P. latens* population in the spraying parcel; CK is the reduced rate of *P. latens* population in the blank parcel.

2.3 Environmental information monitoring

Environmental information was the important data that need to be obtained in the experiments. In the UAV spraying, the droplet deposition effect would be affected by environmental factors, such as temperature^[24], humidity^[25], and wind speed^[26]. Therefore, dynamic environmental factors need to be input into the decision model. The SHT35 temperature and humidity sensor (Sensirion, Switzerland) was used to monitor temperature and humidity information. Its temperature measurement range was from -40.0 °C to 125.0 °C, and the humidity measurement range was from 0% RH to 100% RH. Moreover, the temperature measurement accuracy was (± 0.2) °C, and the humidity measurement accuracy was (± 1.5)% RH. The wind speed sensor (Openjumper, China) in the measurement range from 0 to 55.6 m/s was used to monitor wind speed information in the experimental parcels, and the measurement accuracy was (± 0.2) m/s. In experimental task 1, sensors were installed in the center of each block in the five parcels. In experimental task 2, sensors were installed in the center of the ASDS parcel.

2.4 Crop information monitoring

In experimental task 1, the canopy coverage pictures of the crops need to be taken to analyze the LAI, which is a key parameter for the decision model. The measurement system of winter wheat LAI based on the Android mobile platform^[27] that was developed by the Key Laboratory of Modern Precision Agriculture System Integration Research was used to analyze the LAI of each block in the five parcels. When taking canopy coverage pictures, an auxiliary viewfinder frame with a size of 50 cm×50 cm was used to determine the photo area, and a whiteboard with a size of 5 cm×5 cm was placed in the photo area as a reference. Five sampling points under the UAV route were selected randomly in each block to take photos and the LAI values of five sampling points were averaged as LAI of this block to reduce the random errors. In experimental task 2, five pictures were taken at random locations of each block in the ASDS and conventional parcels to calculate the average LAI of this block by the measurement system of winter wheat LAI based on the Android mobile platform. In addition, the growth days of wheat were recorded in each experiment.

2.5 Droplets collection and analysis

In the two experimental tasks, the deposition of droplets after spraying was analyzed. A stalk of wheat was chosen in each photo area, and the water-sensitive papers (WSPs) (Syngenta, Switzerland) were fixed on the upper, middle, and lower layers of the wheat canopy and the ground below the wheat (Figure 3). The WSPs were cut into 1 cm×8 cm to fix the WSPs on the wheat leaves conveniently. Two pieces of WSP were fixed on each layer to determine the droplet deposition on both sides of the leaves. After spraying, the WSPs were collected and analyzed using a high-resolution scanner (Epson, Japan) and Deposit Scan software (Application Technology Research Unit, USA) to obtain droplet deposition data. In experimental task 1, all the droplet deposition data (5 sampling points×6 positions of a wheat plant) on the wheat canopy of each block were averaged as the average droplet deposition of this block. In experimental task 2, to evaluate fully

the droplet deposition effect of the decision results of the ASDS, the average droplet deposition was calculated, and the deviation between the average and theoretical droplet depositions was determined according to the root-mean-square error (RMSE, Equation (3)). The uniformity of the deposited droplets and the penetrability of the droplets also need to be evaluated. The coefficient of variance (CV, Equation (4)) can be used to measure the uniformity of the deposited droplets in the same layer at different sampling points in the horizontal space and the penetrability of the droplets at different layers at the same sampling point in vertical space^[28]. The smaller the value of CV is, the better the uniformity of the deposited droplets and the penetrability of the droplets.

$$\text{RMSE} = \sqrt{\frac{1}{n} \sum_{i=1}^n (X_i - X_T)^2} \quad (3)$$

$$\text{CV} = \frac{S}{\bar{X}} \times 100\% \quad (4)$$

$$S = \sqrt{\frac{1}{n-1} \sum_{i=1}^n (X_i - \bar{X})^2} \quad (5)$$

where, n is the number of blocks; X_i is the average droplet deposition of a block; X_T is the theoretical average droplet deposition of the parcel; S is the standard deviation of the droplet deposition; \bar{X} is the average value of the average droplet deposition of all blocks.

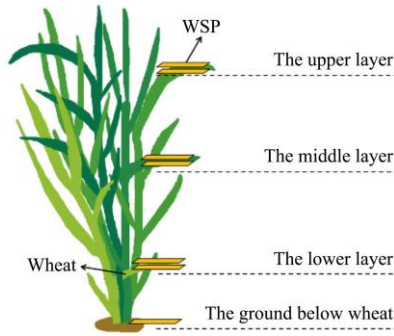


Figure 3 Deployment sketches of collecting droplet deposition

3 Modeling and design of the system

3.1 Evaluation criteria for the decision model according to the optimal coverage method

The premise of decision-making is to ensure the control efficacy of pesticides, which is influenced by canopy pesticide depositions. Therefore, effective pesticide droplet deposition on the canopy needs to be determined for the target crop, which is used as the evaluation criteria for the decision model in the ASDS^[29]. The optimal coverage method that was described by Gil et al.^[30] showed the calculation of the theoretical spraying volume rate based on LAI and droplet deposition on the target^[30]. On the basis of the optimal coverage method, an equation that is used to calculate the effective theoretical droplet deposition is obtained as follows:

$$V_D = \frac{V_T}{2 \cdot \text{LAI}} E \times 10^{-2} \quad (6)$$

where, V_D is the theoretical average droplet deposition on the target, $\mu\text{L}/\text{cm}^2$; V_T is the conventional volume rate to be applied, L/hm^2 ; LAI is the leaf area index of the parcel, m^2/m^2 ; E is the application efficiency.

The pesticide was effectively applied as droplets were deposited on the target. The application efficiency in Equation (6)

is the proportion of total droplet volume on the target to the spraying volume of the pesticide, which is influenced by spraying losses, such as airborne spraying drift and soil deposition of the pesticide^[31]. The control efficacy of the pesticide was weakened by spraying losses, and additional pesticide liquid needed to be sprayed^[32]. Given that the ASDS needs to make sufficient droplet deposition on the crop canopy to ensure control efficacy, all pesticide droplets were assumed to deposit on the target theoretically, and E was set to 1.

The decision-making is based on the theoretical droplet deposition calculated by the optimal coverage method, and the UAV spraying parameters are deduced. Droplet deposition is affected by many factors, including UAV spraying parameters, crop information, and environmental information, and a droplet deposition prediction model was designed. According to the current environment and crop conditions, combined with the droplet deposition prediction model, the spraying decision model provides the optimal UAV spraying parameters to make the predicted droplet deposition as close as possible to the theoretical droplet deposition (Figure 4).

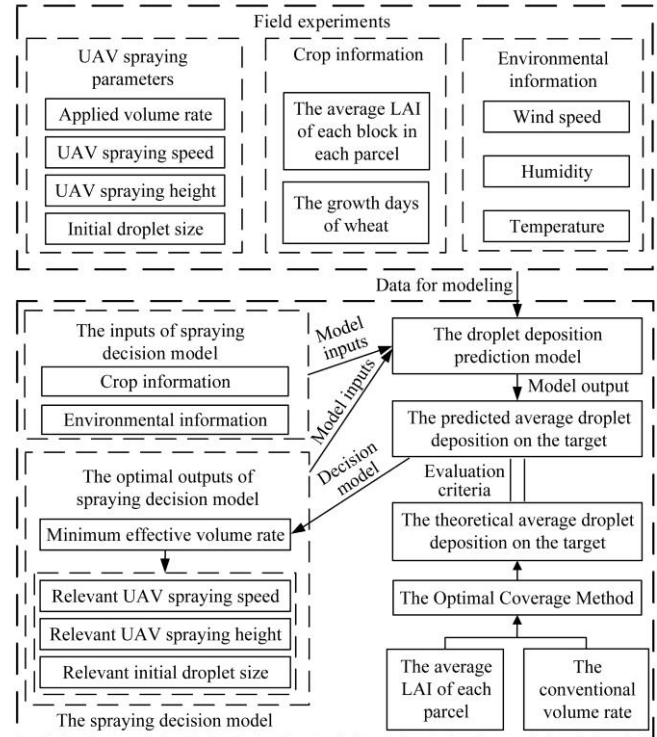


Figure 4 Block diagram of decision making

3.2 Architecture of the spraying decision model based on the RL algorithm

The RL algorithm based on the actor-critic network structure was used to design the spraying decision model. The algorithm combines the advantages of policy gradient and function approximation. The actor-network is based on the probability to select model outputs. The critic network judges the score based on the behavior of the actor-network, and the actor-network modifies the probability of the outputs based on the score of the critic network. The actor-critic network structure can be updated in a single step and achieve fast convergence^[33].

A performance index function must be established in designing the spraying decision model to evaluate the gap between the predicted droplet deposition and the theoretical droplet deposition calculated from the optimal coverage method and whether or not the model output is optimal. The performance index function is

approximated through the critic network, which is used as the standard for obtaining the optimal UAV spraying parameters. The actor-network is used to fit the correspondence between crop and environmental information and UAV spraying parameters, and the critic network is used to replace the traditional output error to update the weight of the actor-network. This procedure ensures that the final output meets the target of the spraying decision model.

In this study, 3840 sets of field data (i.e., 4 growth stages \times 5 wheat varieties \times 6 applied volume rates \times 32 orthogonal combinations of other spraying parameters) were used for modeling. The input of the spraying decision model is $i_d=[L, N, T, H, W]^T$, where L is the leaf area index; N is the growth days of wheat, d; T is the initial value of temperature, °C; H is the initial value of humidity, %RH; W is the wind speed, m/s. The output of the model is $o_d=[q, d, v, h]^T$, where q is the applied volume rate, L/hm²; d is the initial droplet size, μm ; v is the spraying velocity, m/s; h is the spraying height, m.

3.2.1 Design process of the droplet deposition prediction model

A droplet deposition prediction model was designed based on the three-layer back propagation (BP) neural network to predict the average droplet deposition of the canopy according to the current input and output. The input of the droplet deposition prediction model is $i_p=[L, N, T, H, W, q, d, v, h]^T$, and the output is the average droplet deposition of the canopy. The field data set for the spraying decision model was also used to train the BP neural network. The data set was divided into 3000 groups as the training set and 840 groups as the test set. The number of neurons in the input layer was 25, the number of neurons in the hidden layer was 10, the number of neurons in the output layer was 1, the activation function was the rectified linear unit, and the learning rate of the neural network was 0.1. The droplet deposition prediction model participated in training the critic network of the spraying decision model.

3.2.2 Design process of the critic network

To establish the optimal performance index function, the critic network was designed^[34]. Before establishing the performance index function, the error function e is defined as follows:

$$e = X_T - X \quad (7)$$

where, X is the predicted average droplet deposition of the canopy from the droplet deposition prediction model; X_T is the theoretical droplet deposition.

The performance index function $J(e)$ is defined as follows:

$$J(e) = \int_0^{\infty} r(e(s), o_d(s)) ds \quad (8)$$

where, $r(e, o_d) = e^2 Q_1 + o_d^T Q_2 o_d$ is the utility function, $Q_1 \in \mathbb{R}$ is a positive constant, and $Q_2 \in \mathbb{R}^{4 \times 4}$ is a diagonal constant matrix.

On the basis of the definition of the performance index function $J(e)$, the Hamiltonian function $H(e, o_d)$ is defined as follows:

$$H(e, o_d) = r(e, o_d) + \nabla J^T \dot{e} \quad (9)$$

where, $\nabla J = \frac{\partial J(e)}{\partial e} \in \mathbb{R}$ is the gradient of the performance index function J .

When the error function e is minimum, the optimal performance index function $J^*(e)$ can be obtained:

$$J^*(e) = \min \int_0^{\infty} r(e(s), o_d(s)) ds \quad (10)$$

The optimal performance index function $J^*(e)$ also satisfies the Hamilton-Jacobi-Bellman equation as follows:

$$H(e, o_d^*) = r(e, o_d^*) + \nabla J^{*T} \dot{e} = 0 \quad (11)$$

where, $\nabla J^* = \frac{\partial J^*(e)}{\partial e} \in \mathbb{R}$ is the gradient of the optimal performance index function J and o_d^* is the optimal output of the model.

The target of the spraying decision model is to obtain the optimal output o_d^* through the RL algorithm based on the actor-critic network structure when the input i_d is known.

The optimal performance index function $J^*(e)$ can be approximated by the following neural network:

$$J^*(e) = \omega_c^T \varphi_c(e) + \varepsilon_c(e) \quad (12)$$

where, $\omega_c \in \mathbb{R}^{N_c}$ is the ideal weight matrix of the neural network; $\varphi_c(\cdot) \in \mathbb{R}^{N_c}$; $\varepsilon_c(\cdot) \in \mathbb{R}$ are the activation function and the approximation error of the neural network, respectively; N_c is the number of neurons of the neural network. The activation function $\varphi_c(\cdot)$ is selected as the hyperbolic tangent function $\tanh(\cdot)$.

The differential form of the optimal performance index function $J^*(e)$ is obtained as

$$\nabla J^* = \nabla \varphi_c^T(e) \omega_c + \nabla \varepsilon_c(e) \quad (13)$$

where, $\nabla \varphi_c = \frac{\partial \varphi_c}{\partial e} \in \mathbb{R}^{N_c}$, $\nabla \varepsilon_c = \frac{\partial \varepsilon_c}{\partial e} \in \mathbb{R}$. The approximation of the optimal performance index function $\hat{J}(e)$ based on the critic network is designed as follows:

$$\hat{J}(e) = \hat{\omega}_c^T \varphi_c(e) \quad (14)$$

where, $\hat{\omega}_c(t)$ is the estimation matrix of the ideal weight matrix ω_c of the neural network.

The matrix $\hat{\omega}_c(t)$ is chosen to minimize the objective function $E_c = \frac{1}{2} e_c^2$ and $e_c(\cdot)$ is the approximation of the Hamilton function, which can be expressed as

$$e_c = e^2 Q_1 + o_d^T Q_2 o_d + \hat{\omega}_c^T \nabla \varphi_c \dot{e} \quad (15)$$

The updating law for the critic network can be obtained as

$$\dot{\hat{\omega}}_c = -a_c \sigma_c (\sigma_c^T \hat{\omega}_c + e^2 Q_1 + o_d^T Q_2 o_d) \quad (16)$$

where, $a_c \in \mathbb{R}$ is the learning rate of the critic neural network, and the auxiliary function σ_c is defined as $\sigma_c = \frac{\sigma}{\sigma^T \sigma + 1} \in \mathbb{R}^{N_c}$ with

$$\sigma = \nabla \varphi_c \dot{e} \in \mathbb{R}^{N_c}.$$

3.2.3 Design process of the actor-network

The performance index function from the critic network was input into the actor-network for updating weight, and the decision output was given by the actor network^[35]. The output $o_d(i_d)$ of the model can be approximated by the following neural network

$$o_d(i_d) = \omega_a^T \varphi_a(i_d) + \varepsilon_a(i_d) \quad (17)$$

where, $\omega_a \in \mathbb{R}^{N_a}$ is the ideal weight matrix of the neural network, and $\varphi_a(\cdot) \in \mathbb{R}^{N_a \times 4}$, and $\varepsilon_a(\cdot) \in \mathbb{R}^4$ are the activation function and the approximation error of the neural network, respectively. N_a is the number of neurons in the neural network. The activation function $\varphi_a(\cdot)$ was selected as the hyperbolic tangent function $\tanh(\cdot)$.

The approximation of model output $o_d(i_d)$ based on the actor-network is designed as follows:

$$\hat{o}_d(i_d) = \hat{\omega}_a^T \varphi_a(i_d) \quad (18)$$

where, $\hat{\omega}_a(t)$ is the estimation matrix of the ideal weight matrix ω_a of the neural network.

The error estimation function $e_a(\cdot)$ can be expressed as

$$e_a = \hat{\omega}_a^T \varphi_a(i_d) + k_c \nabla \hat{J}(e) \quad (19)$$

where, $\nabla \hat{J} = \frac{\partial \hat{J}}{\partial e} \in \mathbb{R}$ is the estimated gradient value of the performance index function \hat{J} generated by the critic network and $k_c \in \mathbb{R}$ is a positive constant to be designed for the effect of the critic network on the actor-network.

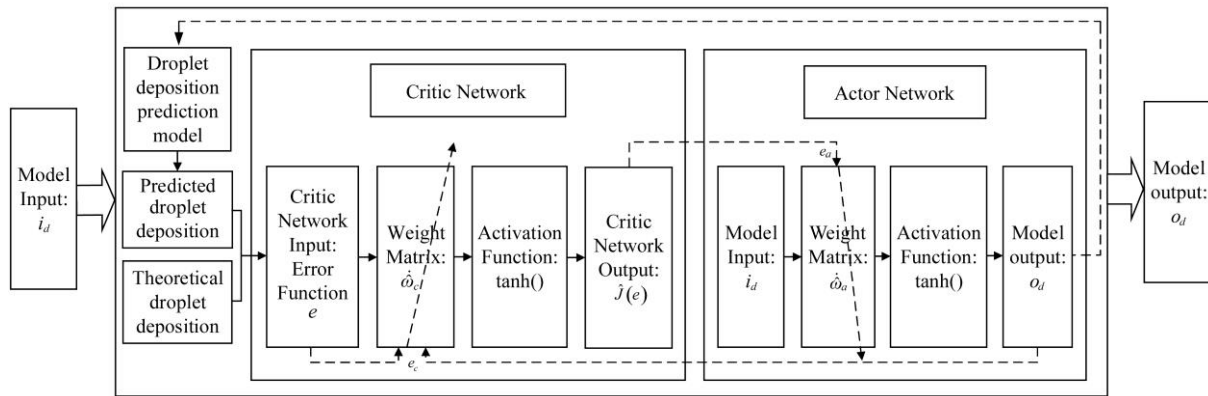
The matrix $\hat{\omega}_c(t)$ is chosen to minimize the auxiliary error estimation function $E_a = \frac{1}{2} e_a^T e_a$, and the updating law for the actor-network can be obtained as

$$\dot{\hat{\omega}}_a = -a_a \varphi_a (\hat{\omega}_a^T \varphi_a + k_c \nabla \varphi_c^T \hat{\omega}_c)^T \quad (20)$$

where, $a_a \in \mathbb{R}$ is the learning rate of the actor neural network.

After the above modeling process, the spraying decision model

based on the RL algorithm based on the actor-critic network structure was established. The architecture of the model consisted of the droplet deposition prediction model, the critic network, and the actor-network (Figure 5). The input i_d of the spraying decision model is the input of the actor-network, and the output o_d of the model is the output of the actor-network. In this model, the critic and actor networks were not independent, and the output of the critic network would participate in the weight updating process of the actor-network, which showed that the value of the performance index function related to the droplet deposition would affect the final weight convergence of the actor-network. The actor-network of the spraying decision model was embedded into the ASDS, and the spraying parameters were recommended for the ASDS parcel of experimental task 2.



Note: The solid line with an arrow represents the forward broadcast process and the dotted line with arrow represents the back propagation process.

Figure 5 Architecture of the designed spraying decision model

3.3 ASDS design

The ASDS was divided into hardware and software parts (Figure 6). The hardware part was composed of sensors and communication nodes, and it was used to obtain real-time environmental information. In specific, Raspberry PI 4B was connected with the SIM7600CE 4G expansion board through a 40-pin GPIO interface as the communication node of the ASDS. The SHT35 temperature and humidity sensor and the wind speed sensor were connected to the communication node through I²C, and a 1 kΩ electric resistance was paralleled between the analog port and the grounding terminal of the communication node, which was used to guide the reference level of the grounding terminal to the measurement port. This setup was established to avoid the interference of the port suspension on the measurement accuracy. Two sensors were fixed on the metal stick, which was inserted in the parcel to collect the temperature, humidity, and wind speed information in the environment.

The software part consisted of a type of Android mobile client software and a cloud server. The functions of the software included obtaining data on the LAI, the number of growth days, and environmental parameters and providing decision suggestions (Figure 7). In this study, the measurement system of winter wheat LAI based on the Android mobile platform mentioned in Section 2.4 was added to the ASDS to obtain the LAI data. The environmental information obtained from the hardware part of the ASDS was sent to the MySQL database of the Tencent cloud server through a 4G network. The Android mobile client software with the MySQL connector Java package can access the MySQL database. When the experimental group was added to the client software, it can obtain the current time of the mobile phone automatically and parse it into the standard data format to calculate

the crop growth days. Meanwhile, the Mobile TensorFlow SDK was added to the Android project to realize the spraying decision model based on the RL algorithm running on the mobile phones.

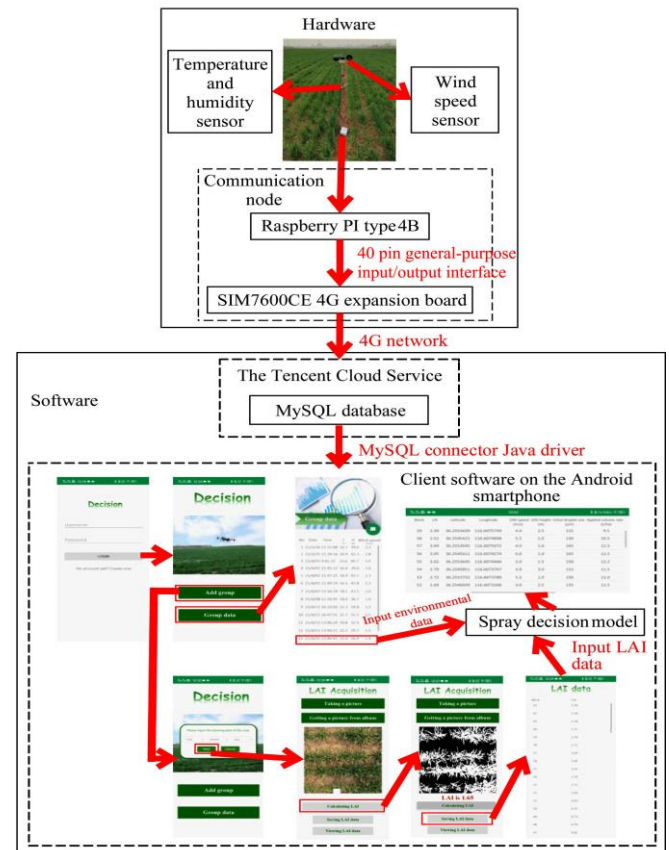


Figure 6 Design structure of ASDS

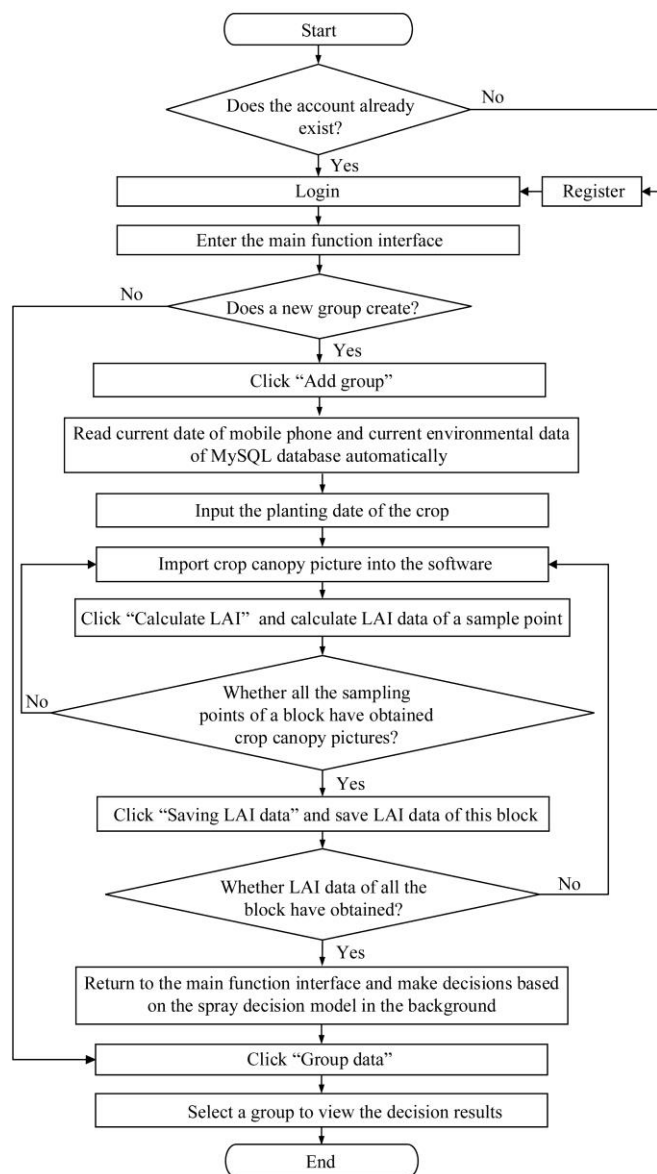


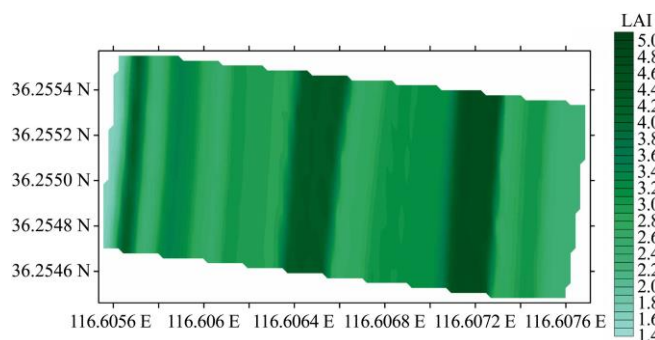
Figure 7 Application flow chart of software part

4 Results and discussion

4.1 Decision results from ASDS

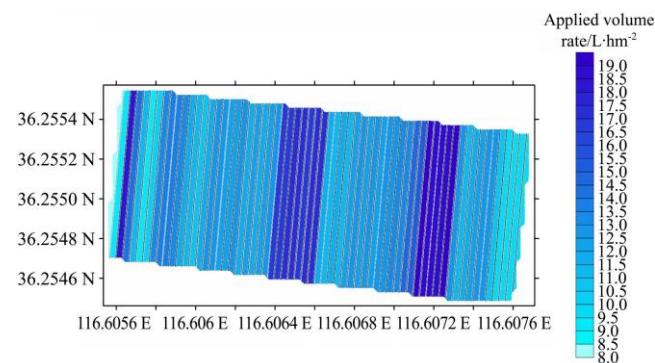
The wheat LAIs of the ASDS parcel in experimental task 2 are shown in Figure 8, which were within the value range of 1.4-5.0, and the average LAI in the whole ASDS parcel was 3.237. Figure 8 shows that the LAIs in different wheat ridges had obvious differences in the same parcel, which may be caused by multiple factors. For example, such factors may include the differences of soil-based fertilizer^[36], moisture distribution caused by geographical relief^[37], and seed depth influenced by soil texture^[38]. In this study, the theoretical droplet deposition under an LAI of 3.237 was used as the evaluation criteria for decision-making.

The ASDS was used to make the decision on the spraying parameters, and recommended decision results according to the LAI in each block were given distinctly in the ASDS parcel (Figure 9). As shown in Figure 8 and Figure 9a, the spraying volume rate was lower in the blocks with higher LAI. In the same parcel, the minimum spraying volume rate was 8.0 L/hm². As for the blocks with higher LAI, the spraying volume rate was higher, and the highest reached 19.0 L/hm², which was more than the traditional spraying volume rate. The overall spraying volume was 26.493 L in the whole ASDS parcel, and the average spraying volume rate

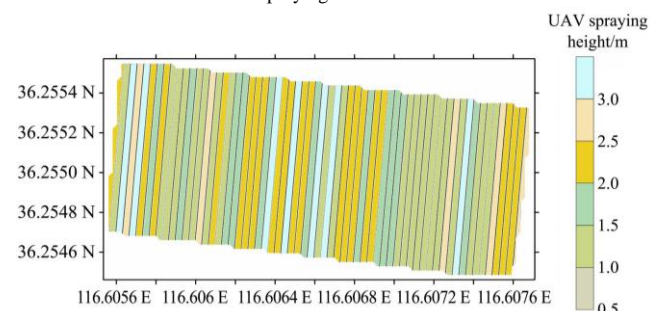


Note: LAI: Leaf area index; ASDS: Adaptive spraying decision system. The same as below.

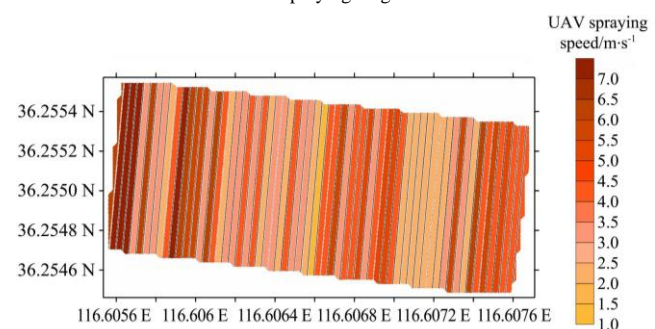
Figure 8 Distribution map of the LAI in the ASDS parcel



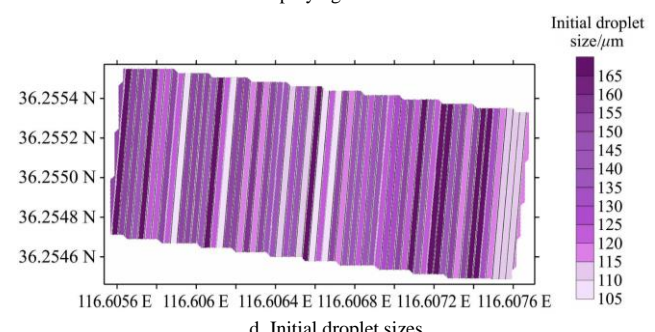
a. Spraying volume rates



b. Spraying heights



c. Spraying velocities



d. Initial droplet sizes

Figure 9 Distribution map of the decision results in the ASDS parcel, where the recommended spraying parameters of 63 blocks were given

was 12.9 L/hm². Compared with the conventional spraying volume rate of 15.0 L/hm², the decision results of ASDS could reduce the spraying volume rate of the pesticide by 14% in experimental task 2. As shown in Figure 9b, the recommended spraying height given by the ASDS was within 1-3 m, with a quite lower height. This result indicated that the lower spraying height can realize a better spraying effect while UAV spraying. Zhang et al.^[28] also showed that the droplets of the pesticide were more likely to drift at a higher spraying height and the droplets could hardly reach the targeted crop. In experimental task 2, the spraying velocity given by ASDS was 2-4 m/s at a medium level (Figure 9c). Kharim et al.^[10] showed that at a flight velocity of 2-6 m/s, the faster the flight velocity of the UAV, the less the droplet deposition. However, Chen et al. explained that at a slower spraying velocity, the UAV spraying would present poor droplet deposition effect on the targeted crop under the influence of strong downwash airflow^[39]. Therefore, the UAV spraying velocity must be set in a reasonable range to improve droplet deposition. As shown in Figure 9d, no obvious regular pattern was observed in setting the initial droplet size. Moreover, Zhang et al. reported that the ideal range of setting droplet size for improving droplet deposition is 50-300 μm^[41]. High-speed atomizing nozzles were installed on the UAV used in this study; therefore, the setting value of the initial droplet size was small^[40]. The initial droplet size given by the ASDS was within 105-165 μm, which was in the ideal range. Although it showed no obvious regular pattern, the initial droplet size also contributed to obtaining theoretical droplet deposition.

4.2 Droplet deposition in the crop canopy

The droplet deposition effect was analyzed after UAV spraying in the ASDS and conventional parcels. In specific, the average droplet deposition was calculated on all sampling points of the wheat canopy in each block, the back side of the leaves, and the upper, middle, and lower layers of the canopy. Afterward, the droplet deposition effect was visualized (Figure 10). The theoretical droplet deposition was calculated as 0.020 μL/cm² based on the average LAI value of 3.237 of the ASDS parcel. The average droplet deposition in each block of the ASDS parcel was within the range of 0.016-0.023 μL/cm², and fluctuations possibly occurred at the level of 0.020 μL/cm². However, as shown in Figure 10a, over 70% of average droplet deposition on all sampling points of the wheat canopy was within the error range of 10% of the theoretical droplet deposition. Thus, the application of ASDS for UAV spraying can make the droplet deposition closer to the theoretical droplet deposition to a great extent, which could guarantee the UAV spraying effect while reducing spraying volume. Figure 10b shows the distribution of droplet deposition at the back side of the leaves. On the basis of the overall values, the average droplet deposition at the back side of the leaves was lower than the average droplet deposition on all sampling points of the wheat canopy. Although the downwash airflow of the UAVs might turn over the leaf and make the droplet deposition at the back side of the leaf reach the average level of the wheat canopy in some blocks, the droplet deposition effect at the back side of the leaf was generally poor. Figure 10c shows the droplet deposition distribution on the upper, middle, and lower layers of the wheat canopy and the ground. Within the ASDS parcel, the upper layer had the highest droplet deposition, whereas the middle and lower layers had less droplet deposition. However, no distinct difference in droplet deposition was found between the middle and lower layers. In addition, droplets were deposited on the WSPs

that were placed on the ground. This result indicated that UAV spraying cannot avoid ground losses and might influence the application efficiency of pesticides in general. This problem will be considered in further research, and the spraying decision model will be optimized to minimize UAV spraying losses as much as possible.

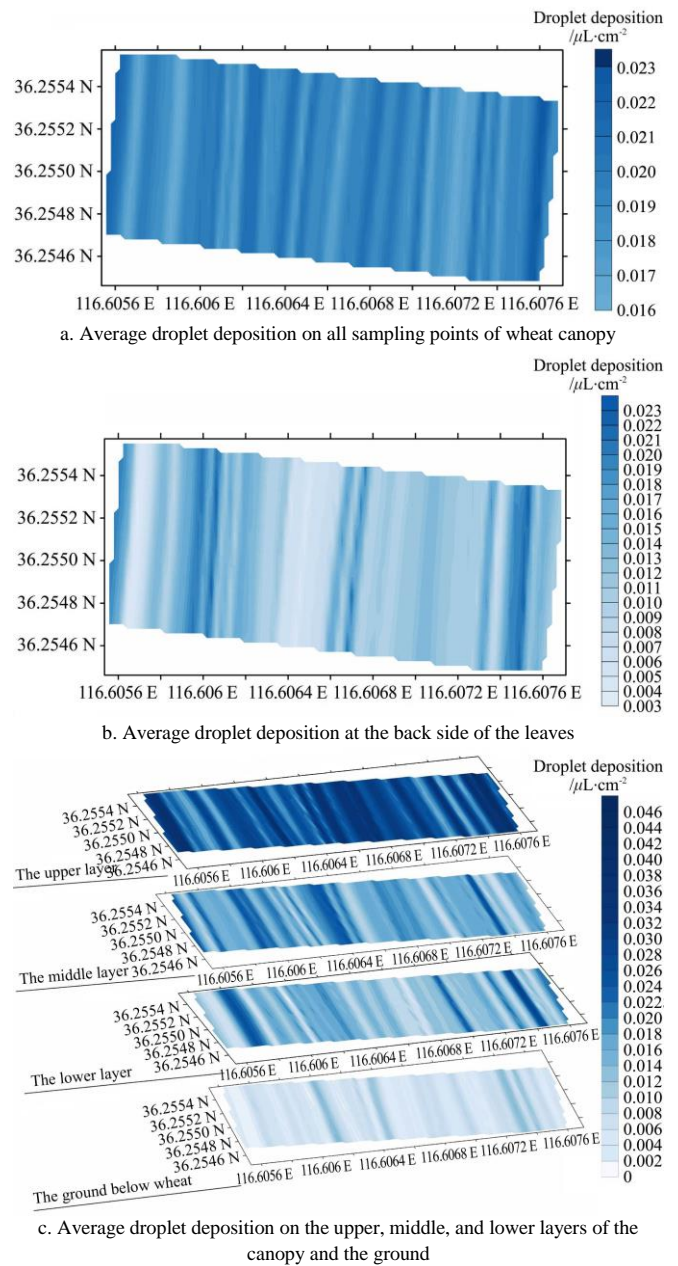


Figure 10 Distribution map of the droplet deposition in the ASDS parcel

Figure 11 shows the LAI distribution in the conventional block. Figure 12 displays the average droplet deposition on all sampling points of the wheat canopy in each block, the back side of the leaves, and the upper, middle, and lower layers of the canopy and the ground. As shown in Figures 11 and 12, obvious relativity was found between the droplet deposition and the LAI when a single parameter combination was used for UAV spraying. The higher the LAI is, the lower the droplet deposition. Such a result was consistent with the result of Zhang^[26]. In this study, the droplet depositions of the ASDS and conventional parcels were compared in Table 3. Although the average droplet depositions of the two parcels on all sampling points of the wheat canopy presented no great difference, the RMSEs of the average and

theoretical droplet depositions in these two parcels showed that the deviation value of the ASDS parcel was smaller. Meanwhile, the ground losses in the ASDS parcel were reduced. Table 4 shows that the droplet deposition on the wheat leaves in the ASDS parcel had better uniformity than that in the conventional blocks. In particular, the average droplet deposition on all sampling points of the wheat canopy had the best result, with the smallest CV and best uniformity. The reason was that the average droplet deposition on all sampling points of the wheat canopy was used to close to the theoretical droplet deposition while establishing the decision model. In addition, the droplet deposition effect after UAV spraying in the OSDS parcel was greatly influenced by the spraying decision model. However, differences in droplet distribution were found in the different canopy layers. As a result, such a problem will be taken into consideration for further improvement of the model. In general, UAV spraying according to the recommended parameters

of the ASDS can save the spraying volume rate, improve droplet deposition, and reduce ground losses.

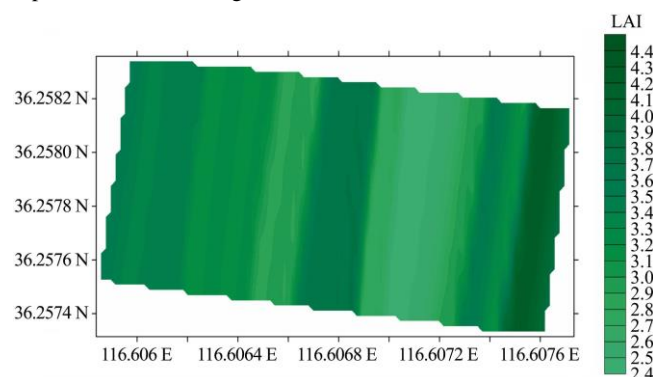
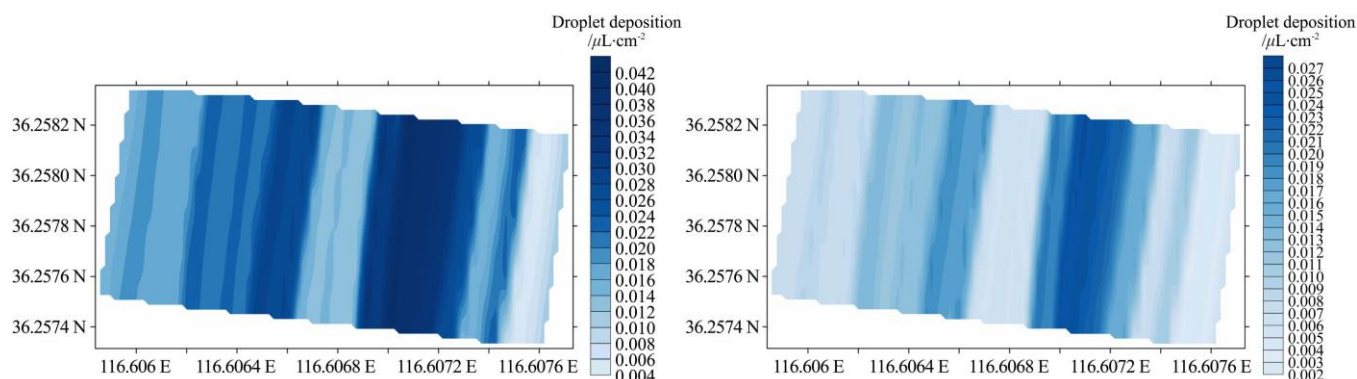
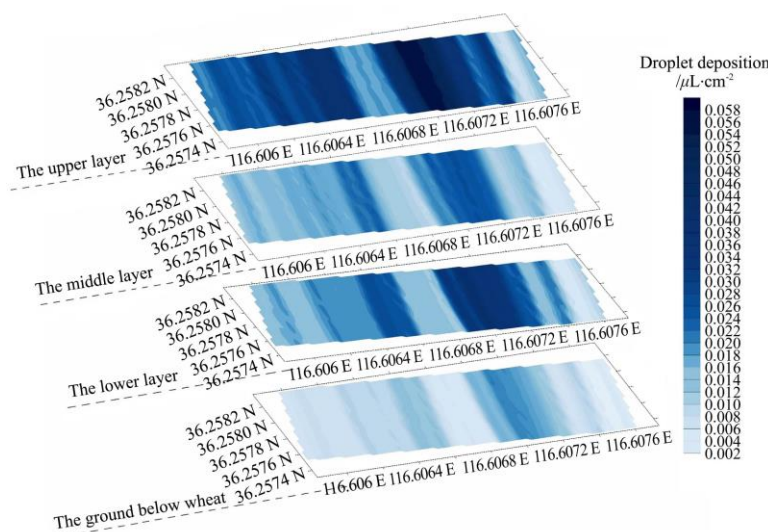


Figure 11 Distribution map of the LAI in the conventional parcel



a. Average droplet deposition on all sampling points of wheat canopy

b. Average droplet deposition at the back side of the leaves



c. Average droplet deposition on the upper, middle, and lower layers of the canopy and the ground

Figure 12 Distribution map of the droplet deposition in the conventional parcel

Table 3 Average droplet depositions and the RMSEs in the ASDS and conventional parcels

Parcels	Average droplet deposition/ $\mu\text{L cm}^{-2}$						RMSEs*
	Total layers	Upper layer	Middle layer	Lower layer	Back side of the leaf	Ground below the wheat	
ASDS parcel	0.019	0.027	0.016	0.014	0.012	0.006	0.002
Conventional parcel	0.022	0.030	0.015	0.021	0.012	0.009	0.009

Note: *RMSEs between the true and theoretical average droplet depositions.

Table 4 Uniformity of the deposited droplets and the penetrability of the droplets in the ASDS and conventional parcels

Parcels	Uniformity of the deposited droplets/%						Penetrability of the droplets/%
	Average	Upper layer	Middle layer	Lower layer	Back side of the leaf	Ground below the wheat	
ASDS parcel	8.8	29.8	34.9	41.1	38.3	54.4	29.6
Conventional parcel	40.9	42.1	39.2	43.6	52.6	52.5	28.4

4.3 Evaluation of control efficacy

The results in Sections 4.1 and 4.2 showed that the ASDS helped reduce the spraying volume and improve droplet deposition. As the main purpose of UAV spraying was for pest control, this section explored whether or not the application of recommended spraying parameters given by the ASDS will influence the control efficacy of UAV spraying. As shown in Table 5, *P. latens* were still of great amount on the seventh day in the blank parcel with no spraying. Thus, the number of *P. latens* cannot reduce spontaneously without spraying for prevention during the experiment. After UAV spraying in the ASDS and conventional parcels, the population of *P. latens* was controlled. On the seventh day after UAV spraying, the reduced rate of *P. latens* population and the control efficacy reached the highest level and

the control efficacy in the two parcels exceeded 98%. The results of the investigations revealed no great differences in control efficacy between the ASDS and conventional parcels. Therefore, following the spraying parameters recommended by the ASDS will not influence the control efficacy of the pesticides. As a result, the use of the ASDS to guide UAV spraying can help reduce the spraying volume rate of the pesticides by 14% in experimental task 2 while ensuring the control efficacy of pesticides, suggesting that this system is valuable for further research. At present, the ASDS can ensure that the control efficacy of the pesticide is similar to that under conventional spraying parameters. In the future, this study will focus on adjusting UAV spraying parameters to improve the control efficacy of the pesticides on the basis of the results of the ASDS.

Table 5 Reduced rates and control efficacy in the ASDS and conventional parcels

Parcels	Population** (ind.)	1 day after spraying		3 days after spraying		7 days after spraying	
		Reduced rate/%	Control efficacy/%	Reduced rate/%	Control efficacy/%	Reduced rate/%	Control efficacy/%
ASDS parcel	632	67.6	65.3	91.5	91.2	98.1	98.0
Conventional parcel	668	70.2	68.1	90.7	90.4	98.8	98.7
Blank parcel	625	6.6	--	3.0	--	4.3	--

Note: **Population per 100 wheat plants before spraying.

5 Conclusions

1) In this study, the ASDS was developed for UAV spraying. This system was composed of environmental information monitoring sensors, a communication node, a cloud service database, an Android mobile client software, and a spraying decision model based on the RL algorithm with the actor-critic network structure. The minimum UAV spraying volume rate and reasonable UAV spraying velocity, UAV spraying height, and initial droplet size were recommended by the ASDS based on the crop and environmental information.

2) Field data were collected from five varieties of wheat in four growth stages for modeling. The theoretical droplet deposition was calculated using the optimal coverage method as the evaluation criteria for the decision model. The model was built by training the critic and actor networks to achieve adaptive decision-making in a complex environment.

3) The spraying parameters recommended by the ASDS were used to spray the wheat parcel, and results showed that the ASDS can adjust spraying parameters according to the LAIs of the parcel. Moreover, the blocks with lower LAI correspondingly had lower spraying volume rates. For experimental task 2 in this study, the ASDS could reduce the spraying volume rate by 14% compared with using the traditional parameters and thus can minimize pesticide use.

4) Compared with the spraying effect under the conventional parameters, the RMSE between droplet deposition and theoretical droplet deposition was smaller, and the uniformity of the deposited droplets improved after UAV spraying on the basis of the ASDS. Moreover, no distinct difference in the penetrability of the droplets and the control efficacy was found between the two treatments. Thus, the ASDS can reduce the spraying volume rate without influencing the spraying effect and control the efficacy of pesticides. Therefore, the ASDS is worthy of further research and improvement.

Acknowledgements

This study was financially supported by the Chinese National

Key Research and Development Plan (Grant No. 2019YFE0125500).

[References]

- [1] Hong S W, Zhao L, Zhu H. CFD simulation of pesticide spray from air-assisted sprayers in an apple orchard: Tree deposition and off-target losses. *Atmospheric Environment*, 2018; 175: 109–119.
- [2] Su X J, Wang Y L, Wei J, Huang C C, Liu A Y, Li S, et al. Pesticide deposition percentage and control effect of nine kinds of crop protection machineries against wheat aphid. *Acta Agriculturae Boreali-Occidentalis Sinica*, 2018; 27(1): 149–154. (in Chinese)
- [3] Li Y N, Wang H D, Qu H R, Cao H Z, Tong B X, Cui S L, Han Y R, Ma W Q. Establishment and assessment of management systems for wheat and maize with high yield and nitrogen use efficiency based on GIS at the village level. *Chinese Journal of Eco-Agriculture*, 2019; 27(7): 1124–1133. (in Chinese)
- [4] Zhang X Q, Song X P, Liang Y J, Qin Z Q, Wu J M. Effects of spray parameters of drone on the droplet deposition in sugarcane canopy. *Sugar Tech*, 2020; 22(2): 583–588.
- [5] Wang C L, Song J L, He X K, Wang Z C, Wang S L, Meng Y H. Effect of flight parameters on distribution characteristics of pesticide spraying droplets deposition of plant-protection unmanned aerial vehicle. *Transactions of the CSAE*, 2017; 33(23): 109–116. (in Chinese)
- [6] Qin W C, Qiu B J, Xue X Y, Chen C, Xu Z F, Zhou Q Q. Droplet deposition and control effect of insecticides sprayed with an unmanned aerial vehicle against plant hoppers. *Crop Protection*, 2016; 85: 79–88.
- [7] Chen S D, Lan Y B, Zhou Z Y, Fan O Y, Wang G B, Huang X Y, et al. Effect of droplet size parameters on droplet deposition and drift of aerial spraying by using plant protection UAV. *Journal of Agronomy*, 2020; 10: 195. doi: 10.3390/agronomy10020195.
- [8] Wang G B, Lan Y B, Qi H X, Chen P C, Hewitt A, Han Y X. Field evaluation of an unmanned aerial vehicle (UAV) sprayer: effect of spray volume on deposition and the control of pests and disease in wheat. *Pest Management Science*, 2019; 75(6): 1546–1555.
- [9] Xue X Y, Tu K, Qin W C, Lan Y B, Zhang H H. Drift and deposition of ultra-low altitude and low volume application in paddy field. *Int J Agric & Biol Eng*, 2014; 7(4): 23–28.
- [10] Kharim M N A, Wayayok A, Shariff A R M, Abdullah A F, Husin E M. Droplet deposition density of organic liquid fertilizer at low altitude UAV aerial spraying in rice cultivation. *Computers and Electronics in Agriculture*, 2019; 167: 105045. doi: 10.1016/j.compag.2019.105045.
- [11] Gil E, Campos J, Ortega P, Llop J, Gras A, Armengol E, et al. DOSAVIA: Tool to calculate the optimal volume rate and pesticide amount in vineyard spray applications based on a modified leaf wall area method. *Computers and Electronics in Agriculture*, 2019; 160: 117–130.

- [12] Tackenberg M, Volkmar C, Dammer K H. Sensor-based variable-rate fungicide application in winter wheat. *Pest Management Science*, 2016; 72(10): 1888–1896.
- [13] Lee R, Uyl R D, Runhaar H. Assessment of policy instruments for pesticide use reduction in Europe; Learning from a systematic literature review. *Crop Protection*, 2019; 126: 104929. doi: 10.1016/j.cropro.2019.104929.
- [14] Chen Y M, Lin F G, Zhao Y, Huang T T, Ding L, Mei A Z, et al. Prevalence reasons and monitoring countermeasures of scab in eastern wheat area of Jiangsu Province. *Plant Diseases and Pests*, 2016; 7(2): 1–6.
- [15] Dong Y Y, Zhao C J, Yang G J, Chen L P, Wang J H, Feng H K. Integrating a very fast simulated annealing optimization algorithm for crop leaf area index variational assimilation. *Mathematical & Computer Modelling*, 2013; 58(3-4): 877–885.
- [16] Bu F, Wang X. A smart agriculture IoT system based on deep reinforcement learning. *Future Generation Computer Systems*, 2019; 99: 500–507.
- [17] An H, Xian B. Attitude reinforcement learning control of an unmanned helicopter with verification. *Control Theory & Applications*, 2019; 36(4): 516–524. (in Chinese)
- [18] Tottman D R, Broad H. The decimal code for the growth stages of cereals, with illustrations. *Annals of Applied Biology*, 1987; 93(2): 441–454.
- [19] Emilia H, Arnoldus W P V. Spray drift review: The extent to which a formulation can contribute to spray drift reduction. *Crop Protection*, 2013; 44: 75–83.
- [20] Tang Y, Hou C J, Luo S M, Lin J T, Yang Z, Huang W F. Effects of operation height and tree shape on droplet deposition in citrus trees using an unmanned aerial vehicle. *Computers and Electronics in Agriculture*, 2018; 148: 1–7.
- [21] Chen W Q. Integrated management of diseases and insect pests on wheat. *Plant Protection*, 2013; 39(5): 16–24. (in Chinese)
- [22] Xiao Q, Li Y P, Li M, Qu T Y, Li D Y, Li X Y. Application of XAIRCRAFT P20 plant protection UAV to the control of *Sclerochloa dura* (L.) Beauv. in a wheat field. *Barley and Cereal Sciences*, 2019; 36(3): 39–40, 51. (in Chinese)
- [23] Ma L, Wang X Z, Wang S P, Liu S T. Evaluation of the control efficiency of lime sulfur to red-spider and main diseases on wheat. *Agrochemicals*, 2016; 55(6): 450–453. (in Chinese)
- [24] Franz E, Bouse L F, Carlton J B, Kirk I W, Latheef M A. Aerial spray deposit relations with plant canopy and weather parameters. *Transactions of the ASAE*, 1998; 41(4): 959–966.
- [25] Maciel C F S, Teixeira M M, Fernandes H C, Zolnier S, Cecon P R. Droplet spectrum at different vapour pressure deficits. *Revista Ciencia Agronomica*, 2016; 47(1): 41–46.
- [26] Fai qal B S, Freitas H, Gomes P H, Mano L Y, Pessin G, Carvalho A, et al. An adaptive approach for UAV-based pesticide spraying in dynamic environments. *Computers and Electronics in Agriculture*, 2017; 138: 210–223.
- [27] Chen Y Q, Yang W, Li M Z, Sun H. Measurement system of winter wheat LAI based on Android mobile platform. *Transactions of the CSAM*, 2017; 48(S1): 123–128. (in Chinese)
- [28] Zhang P, Deng L, Lyu Q, He S L, Yi S L, Liu Y D, Yu Y X, Pan H Y. Effects of citrus tree-shape and spraying height of small unmanned aerial vehicle on droplet distribution. *Int J Agric & Biol Eng*, 2016; 9(4): 45–52.
- [29] Furness G O, Magarey P A, Miller P M, Drew H J. Fruit tree and vine sprayer calibration based on canopy size and length of row: unit canopy row method. *Crop Protection*, 1998; 17(8): 639–644.
- [30] Gil E, Escolà A. Design of a decision support method to determine volume rate for vineyard spraying. *Applied Engineering in Agriculture*, 2009; 25(2): 145–151.
- [31] Jensen P K, Olesen M H. Spray mass balance in pesticide application: a review. *Crop Protection*, 2014; 61(2): 23–31.
- [32] Planas S, Camp F, Solanelles F, Sanz R, Rosell-Polo J R. Advances in pesticide dose adjustment in tree crops. In: 9th European Conference on Precision Agriculture, Lleida, Spain, 2013; pp.533–539.
- [33] Grondman I, Busoniu L, Lopes G A D, Babuska R. A survey of actor-critic reinforcement learning: Standard and natural policy gradients. *IEEE Transactions on Systems, Man, and Cybernetics, Part C (Applications and Reviews)*, 2012; 42(6): 1291–1307.
- [34] Song R, Lewis F, Wei Q, Zhang H G, Jiang Z P, Levine D. Multiple actor-critic structures for continuous-time optimal control using input-output data. *IEEE Transactions on Neural Networks and Learning Systems*, 2015; 26(4): 851–865.
- [35] Fan Q Y, Yang G H. Adaptive actor-critic design-based integral sliding-mode control for partially unknown nonlinear systems with input disturbances. *IEEE Transactions on Neural Networks and Learning Systems*, 2016; 27(1): 165–177.
- [36] Zhang S Q, Zhao S S. Effects of returning whole corn stalk into soil on the soil moisture and manure and winter wheat growth. *Journal of Hebei Agricultural Sciences*, 2001; 5(2): 50–55. (in Chinese)
- [37] Song L, Li F M, Fan X W, Xiong Y C, Wang W Q, Wu X B, Turner N C. Soil water availability and plant competition affect the yield of spring wheat. *European Journal of Agronomy*, 2009; 31(1): 51–60.
- [38] Ibrahim M, Yamin M, Sarwar G, Anayat A, Habib F, Ullah S, et al. Tillage and farm manure affect root growth and nutrient uptake of wheat and rice under semi-arid conditions. *Applied Geochemistry*, 2011; 26: S194–S197.
- [39] Chen S D, Lan Y B, Zhou Z Y, Liao J, Zhu Q Y. Effects of spraying parameters of small plant protection UAV on droplets deposition distribution in citrus canopy. *Journal of South China Agricultural University*, 2017; 38(5): 97–102. (in Chinese)
- [40] Ru Y, Jin L, Zhou H P, Jia Z C. Performance experiment of rotary hydraulic atomizing nozzle for aerial spraying application. *Transactions of the CSAE*, 2014; 30(3): 50–55. (in Chinese)